The Effects of Ink and Media Parameters on Offset Solid Ink and Xerographic Halftoned Image View Quality

Steve Korol
Tektronix Color Printing and Imaging Division
Wilsonville, Oregon

Abstract

Xerographic and offset solid ink technologies are currently dominant in the networked office color printer market. Here, speed, reliability, ease-of-use, cost-per-copy, and image quality are all important factors to the office customer who is often on a tight budget. Both xerography and solid ink have been able to deliver acceptable text output on a wide variety of inexpensive papers; however, such is not always the case for halftoned images. Interestingly, when halftoned image quality fails, it is often for widely different reasons depending on the technology employed.

While offset solid ink exhibits excellent receiver media independence, halftoned images may appear grainy to the customer. Xerographically produced images, on the other hand, are not so often characterized by halftone-induced graininess, but rather by mottle, or image non-uniformity, depending on the characteristics of the receiver media used to generate the output. The focus of the following research is to quantify these characteristics and tie them to specific attributes of the printing systems studied. In order to do so, a relatively recently developed technique is employed for the measurement of image noise, or *granularity*, based on the Wiener (or noise-power) spectrum of the output.[1,2,3] These noise measurements are then correlated to physical phenomena of the printing systems studied. Finally, a simple method based on printing system physical attributes is introduced to estimate the reflection optical density at which maximum granularity occurs.

Introduction

In the networked office color printer market, two technologies are especially common. Xerography (or *electrophotography*), with its substantial history in the office environment, fits well into this arena where speed and cost-per-copy are so important. Offset solid ink technology, a relatively new entry to the market, has made fantastic strides to gain significant market share based on its ease-of-use, ownership cost, and cost-per-copy relative to xerographic machines. While the xerographic and offset solid ink printing mechanisms are entirely different, to the customer, they are the same. In this market, where the output generated by the machines is often used as a tool sell the user's ideas, image view quality is an important attribute, together with the criteria listed above. In order to meet these goals, the successful device must have the ability to print acceptable quality images on a wide variety of substrates reliably. Although both technologies under study generally render text acceptably, each possesses a set of limitations when grayscale images are considered.

In the case of offset solid ink technology, material properties of the ink and the print processing steps within the printer do indeed afford great media flexibility; however, in current implementations of the technology, images may appear grainy to the customer, especially in areas of light optical density (in the range 0.1 to 0.3). The primary reason for this perceived granularity is the minimum diameter and optical density of the smallest achievable mark. Although beyond the scope of this paper, a thorough analysis of the solid ink printing process may be found elsewhere in the literature.[4]

Color xerography, in the networked office color printer market, generally yields images of acceptable image quality on many non-coated papers. It is also generally true, however, that image quality is substantially more dependent on receiver media properties than in the case of offset solid ink technology. It is not altogether uncommon to come across a paper that, aside from the granularity issue mentioned above, yields acceptable image view quality (as differentiated from image *durability* quality, for example) in a solid ink device and unacceptable image view quality in a xerographic device. The converse is very rarely true. While an explanation of the physics of the xerographic process is beyond this paper, there are good examples available.[6,7] The focus instead will be on the effects of these dependencies on halftoned image view quality.

Figure 1 contrasts a 20% digital tint (graylevel 51 out of 256) printed with solid ink technology against xerography. The bitmap used in both cases was generated via the well known *blue noise*, or high frequency weighted noise, technique.[5] Note that in both renderings, although the paper, bitmap, and spatial addressability remained constant between printers, the resulting output is vastly different. Of course, this is to be expected, but it is interesting to analyze the manner in which the two samples differ. The solid ink example is characterized by a fairly homogenous distribution of printed dots of highly uniform size and shape. The xerographic example, on the other hand, is characterized by a minimum mark size apparently much smaller than that of solid ink. Also, the xerographic sample appears to have an undulating low frequency component, that is, the spatial

density of the toner dots varies in a somewhat correlated fashion. It is this latter trait that manifests itself as *mottle* in xerographic prints on some papers.
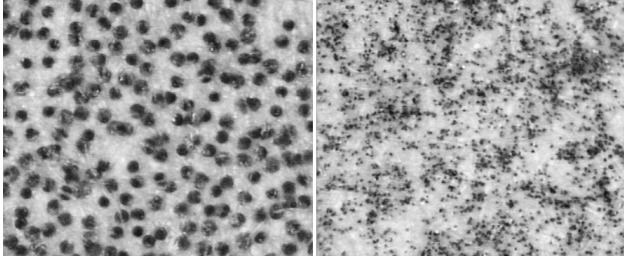
Figure 1: Hardcopy renderings of a 20% digital tint, halftoned using a blue noise mask and printed on a common low cost 20# bond paper. Solid ink at left; xerography at right.

Quantifying Halftoned Image View Quality Differences

To put Figure 1 in context, it should be noted that at normal viewing distance (between 25 and 30 cm for an 8.5"x11" page), the dots printed using solid ink are perceptible, while those of xerography are most commonly not. This point is of great importance, as it is the fundamental reason for the perception of granularity in solid ink prints. The eye's response to frequency may be modeled by the well documented Visual Transfer Function (VTF),[1,2,8] where

$$VTF(u,v) =$$
$$\begin{cases} 5.251e^{-0.7609\sqrt{u^2+v^2}}(1-e^{-0.5236\sqrt{u^2+v^2}}), & \sqrt{u^2+v^2} > 1 \\ 1, & \sqrt{u^2+v^2} \le 1 \end{cases} \quad (1)$$

Figure 2 presents a density plot of the VTF, centered at zero, with limits of plus and minus 15 cycles/mm. Note that although the equation does attenuate frequencies greater than a couple cycles/mm rather aggressively, the image printed in this manuscript will surely appear even more dramatic due to the effects of the printing process.
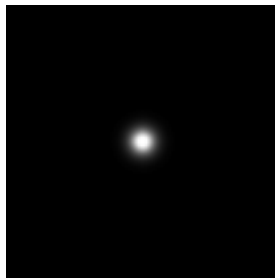
Figure 2: Density plot of the VTF; scale is -15 to +15 cyc/mm.

Given this understanding of the eye's spatial frequency filtering effect, focus turns to the noise content of the image. Following the lead of other researchers in this field, it makes good sense to draw on the efforts of silver halide scientists, as in this research can be found some of the most

robust analyses of image noise. In the classic text by Dainty and Shaw[9], noise in photographic images is modeled as a stationary ergodic process. A stationary process possesses statistics that are the same over all areas of the image, and an ergodic process possesses statistics that can be determined from a single sampling of the image. If these conditions hold, it is possible to show quite conveniently that a measurement of the first order image statistics reveals a good deal about the noise content of the image, especially if the noise distribution is Gaussian.

In the case of image granularity, however, it is necessary to obtain information regarding the *spatial* nature of the image noise. For stationary ergodic processes, the second order probability density function reveals that at any point in the image, the value of the point lies within some discrete delta. Although this second order probability function is generally quite computationally challenging, in the case of a Gaussian distribution, it is completely specified by the autocorrelation function of the image. This result is indeed pleasing, as the Wiener-Khintchin theorem states that the Wiener noise power spectrum and the autocorrelation function are Fourier transform pairs, so

$$W(u,v) = \iint C(\xi,\eta)e^{-2\pi i(u\xi+v\eta)}d\xi d\eta \quad (2)$$
$$C(\xi,\eta) = \iint W(u,v)e^{+2\pi i(u\xi+v\eta)}du dv \quad (3)$$

or more simply,

$$W(u,v) = \Im\left[C(\xi,\eta)\right] \quad (4)$$

where ξ and η are offsets. It is important to underscore the point that in order to take advantage of these conveniences, the images studied must closely approximate stationary ergodic Gaussian processes. If this is the case, there exists a straightforward approach to the computation of perceived image noise, or granularity g. This general method has been applied in the recent past[2] and is given by

$$g = \sqrt{\frac{\int_{-V}^{V}\int_{-U}^{U} W(u,v)VTF^2(u,v)du dv}{\int_{-V}^{V}\int_{-U}^{U} VTF^2(u,v)du dv}} \quad (5)$$

It is important to point out that in keeping with the published technique, images are first cast in terms of reflectance before their statistics are calculated. In practice, the Wiener spectrum may be estimated directly using the well known periodogram approach[5], or by computing the autocorrelation of the image and making use of equation (4). The merits of the latter approach have been presented recently.[2]

The more the images disobey the above constraints of stationarity, ergodicity, and Gaussian behavior, the more questionable the validity of the results. In the following experiments, one blue noise dithering technique was used for all of the samples analyzed. Although a white noise dither would have been statistically more appropriate, visually it

would not have been. While such a blue noise distribution does not strictly abide by the guidelines stated above, in actuality there was found to be sufficient power at all frequencies to yield results of adequate precision.

Figure 3 illustrates the frequency components of two halftone patterns. The top example represents the case of blue noise dithering, with its characteristic attenuation of low frequency detail. In stark contrast, the bottom example represents the case of ordered dithering, characterized by a concentration of energy at low frequency and periodic energy spikes at a rate consistent with the sampling scheme and halftone frequency. From this example, it is obvious that the ordered dither pattern undermines the foundation of the granularity derivation, specifically that images formed using ordered dithers are not random processes by any stretch.
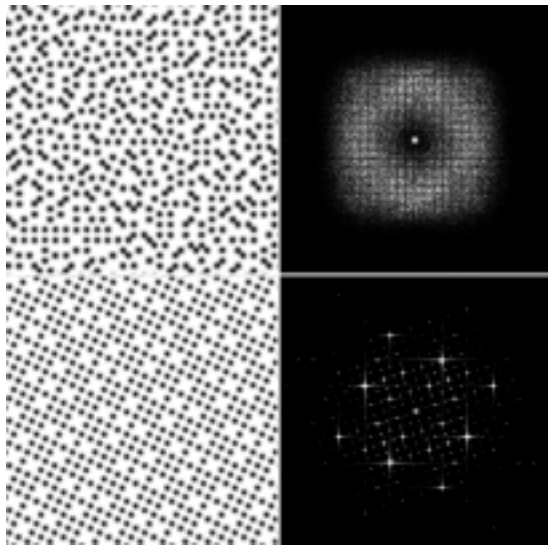
Figure 3: 20% fill halftone patterns and their respective Fourier spectra. Blue noise, top; 30° angled, bottom. Frequency plots on same scale as Figure 2.

It is interesting to note that in actual xerographic printers, the blue noise dithering algorithms common to solid ink systems are not widely used. Rather, dispersed dot and hybrid combinations of dispersed dot and blue noise dithers are used to help mask artifacts induced by the printing mechanism and to compensate for the characteristics of the exposure system. Blue noise dithering was used in the experimentation primarily to maintain alignment with the statistical guidelines, but also to afford simpler comparison between the two printing systems. Although not quantified in this research, visible patterning caused by the dithering methods employed by some xerographic machines can actually decrease image quality.

Please note that in Figure 3, as in all following presentations of frequency data, the results have been transformed by

$$Display(u, v) = c \cdot \log[1 + |F(u, v)|] \qquad (6)$$

as has been previously suggested[10], in order to compress the inherently high dynamic range of frequency plots for display

purposes. The arbitrary constant c has been chosen to yield satisfactory reproductions in this manuscript (hopefully).

Measurement of the Effects of Ink and Media Interaction on Halftoned Image View Quality

Given this metric for the perception of image granularity, it is now possible to quantify some of the effects of ink and media interactions on halftoned image quality. In order to gain an understanding of the quality of a halftoned image, it is critical to make several measurements across the tonal range. Of course, in terms of first order image statistics, this is no new idea and well known techniques allow their straight forward measurement. It has only been fairly recently, though, that it has been so convenient to compute higher order image statistics. To this end, in previous work of note,[2] granularity has been plotted against mean reflectance. Indeed, this is a logical approach based on the computation of granularity in terms of reflectance. Even so, for reasons that will be made clear in the paragraphs to come, in the present research, granularity is plotted against reflection optical density.
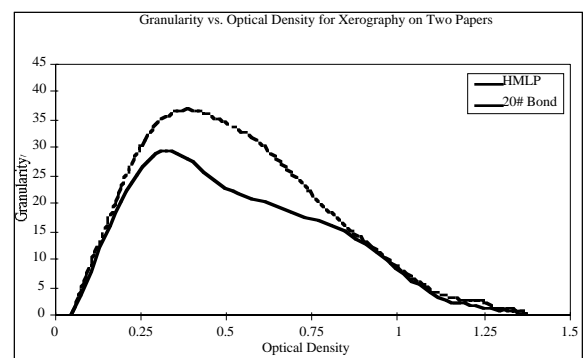
Figure 4: Granularity vs. Optical Density for Xerography. HMLP = Hammermill Laser Print.
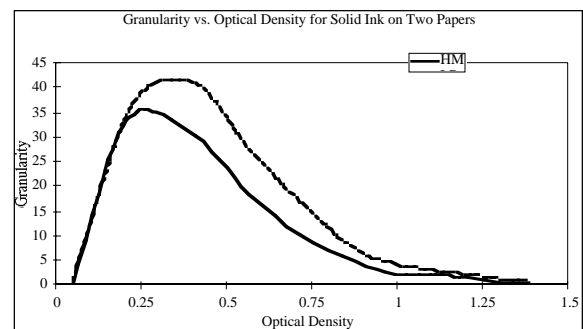
Figure 5: Granularity vs. Optical Density for Solid Ink.

Observations of Media Property Effects

Figures 4 and 5 present image granularity as a function of optical density for xerography and offset solid ink on two papers. First and foremost, note the shape of the curve, with a characteristic maximum between 0.25 and 0.35 optical density units (ODU). Note further the dependence on media

type for the two technologies. In both cases, granularity for the samples printed on a 20# bond copier paper is higher in the low to mid section of the tonal range. The differences were found to be directly attributable to the physical properties of the paper.

Figure 6 contains a set of four images. The top two images were made by transmitting light through un-imaged paper samples. The left-hand sample is *Hammermill Laser Print*; the right-hand sample is 20# bond copier paper. Note the appearance of mottle in the copier paper. It is primarily this fact that leads to an increase in granularity and a corresponding degradation in image view quality. The effects of the differences in the paper on granularity can be observed via the spectral distributions of the halftoned images resulting from their use. The lower two images of Figure 6 are the Fourier spectra of 40% digital halftoned images made with xerography using the papers pictured above. The compressed spectrum of the image printed on 20# bond paper leads to high values for the autocorrelation, and hence, granularity.
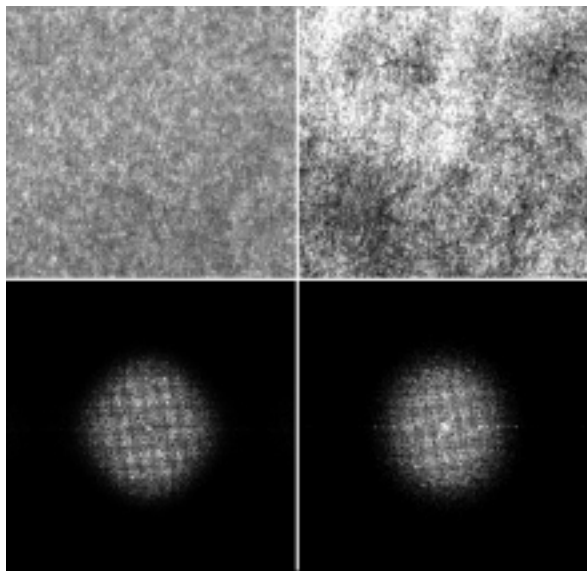
Figure 6: The effect of paper formation on granularity. Upper images are transmission illumination views of HMLP at left and 20# Bond at right. Lower views are Fourier spectra of halftoned images printed on above papers with xerography.

In addition to the effects of paper formation, paper roughness plays a role in high quality xerographic and solid ink printing. Although stated earlier, it is worth pointing out again that current products based on both of these technologies do perform well on several non-coated papers. Even so, especially in the case of xerography, there is a dependency on roughness that can degrade image view quality.

Figure 7 reveals high magnification views of minimum mark size dots printed on *Hammermill Laser Print* paper with both technologies. Through visual analysis of these SEM images, it becomes apparent that as both technologies move to smaller and smaller minimum mark sizes, variations in the surface structure of the receiver media will

play a role of increasing importance to image view quality. This is especially true in the case of xerography, where the marks are actually comprised of a large number of toner particles on the order of 10 μm in diameter. While their nature makes it difficult to print on some surfaces, it also enhances image view quality. As their spatial distribution is roughly Gaussian, the edges of dots are effectively blurred, making detection by the eye more difficult. Dots printed via solid ink technology receive no such benefit, as shown by the SEM images.
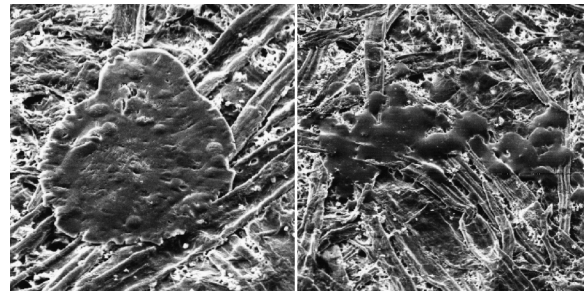
Figure 7: SEM images of single dots on HMLP. Solid Ink at left; xerography at right.

An interesting case in which image view quality is adversely affected by paper structure may be found in the analysis of rough textured papers. Such papers are often used in specialty applications where the aesthetic feel and look of the paper itself is used to convey a certain quality. The textured finishes applied to the sheet during the paper manufacturing process may or may not be periodic over the dimensions of the sheet. It is interesting to point out, that an analysis of such periodic textured patterns using the granularity metric as defined above, strictly speaking, is in violation of the underlying statistical principles. However, it was found via Fourier analysis that although the contribution of the periodic patterning is significant, there is substantial random noise content throughout the sheet. Visual analysis confirms this fact, as xerographic images printed on this paper appear both spatially banded and grainy.

In Figure 8, granularity measurements for such a paper are presented together with those of Figure 4. Although the maximum granularity is not greater for the textured paper (labeled *CC*) than for the bond paper, the high granularity extends much further along the optical density axis. Viewing the samples closely reveals that although the mean density is increasing over this range, higher order statistics (namely the autocorrelation) remains nearly constant. While toner continues to be deposited onto the sheet, its spatial distribution is limited by the structure, random or otherwise, of the rough sheet. This fact is further evidenced by the low maximum optical density on the graph (of sample *CC*). A final observation regarding this material is that under magnification, ink area coverage is substantially incomplete below a density of about 0.75, which is the point where granularity finally begins to decrease. This correlation between granularity and ink area coverage is indeed interesting and worthy of further investigation.

**Granularity vs. Optical Density
For Xerography on Three Papers**
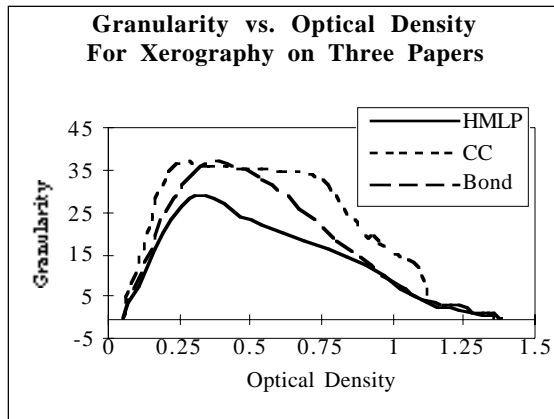
Figure 8: Granularity in xerography on rough, textured paper.

Observations of Ink Property Effects

Due to the fact that the halftoning process involved in the reproduction of solid ink and xerographic images can be modeled as binomial mixing of ink and paper optical densities, it is logical to expect that the maximum variance in image density fluctuation would occur at a point midway between the ends of the tonal scale. While in an idealized grid structure this is indeed the case, most printing technologies, including the solid ink and xerographic processes, are far from ideal. To borrow a term from conventional printing, *dot gain* affects the tone reproduction characteristics of both systems under study. Dot gain may be defined as the physical and optical enlargement of printed dots by the printing system used to generate the output and the measurement system used to quantify it. Figure 9 illustrates the effects of dot gain. While 40% of the pixels in the blue noise halftone array were employed to produce the magnified images shown, the output is in fact much darker. Stated another way, although it was desired that 40% of the page area be printed, much more than 40% area coverage resulted.
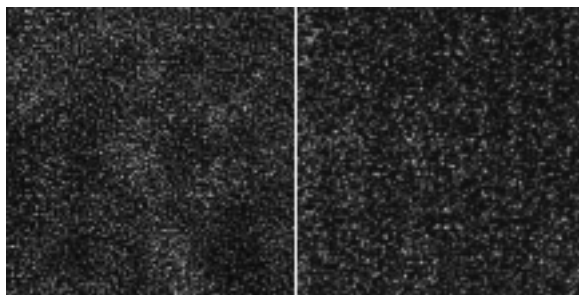
Figure 9: Enlargements of a 40% digital tint printed on 20# bond paper. Solid ink at left; xerography at right.

While optical dot gain effects are common to all hardcopy halftones, physical dot gain effects are specific to the device used to generate the hardcopy. In the case of offset solid ink technology, the ductile ink drops spread a great deal when they are transferred, under heat and pressure, from the intermediate drum to the paper surface. In xerography, dot gain is not induced at the point when toner is brought into contact with the paper; rather, it is during fusing of the image, again under heat and pressure, that physical dot gain occurs.

Due to the dot gain effects inherent in the systems studied, a fairly uniform layer of ink covers the paper well before 100% digital fill is achieved via halftoning. At the point that this uniform layer of coverage is reached, contrast is greatly reduced, and the noise level drops rapidly. At some point prior to this, there is an evenly distributed binomial distribution of dark and light areas on the page. It is at this point that the maximum image noise is expected according to binomial statistics. In order to approximate this point, the well known Yule-Nielsen equation suffices. Cast in terms of optical density, the equation may be written as

$$\%T = 100\left(\frac{1-10^{-Dt/n}}{1-10^{-Ds/n}}\right) \qquad (7)$$

where *%T* is the percent dot area coverage of the sample in question, *Dt* is the optical density of the sample in question, *Ds* is the optical density of an area of solid ink coverage, and *n* is an empirically derived factor relating to the light scattering properties of the ink and paper. As the desire is to determine the optical density at which the noise of the binomial distribution is maximized, equation (7) must be solved for *Dt* at *%T* = 50. Doing so yields

$$Dt_{50} = -n \cdot \log\left[1-\left(\frac{1-10^{-Ds/n}}{2}\right)\right] \qquad (8)$$

In practice, *n* for the paper under study was predetermined. The area at which *Ds* should be taken was determined with the aid of a digital microscope by selecting the dithered region in which there were no spaces between printed dots and minimal overlapping of dots.

Given this measurement and a value for *n* (around 1.5), it was possible to estimate the optical density at the point of maximum noise. Although this estimate is still affected by dot gain, the region over which the dot area is approximated is reduced, thereby reducing error. For the examples given in Figures 4 and 5 above, the error between the measured value and the estimate was found to be less than 7%. The technique is really not applicable to samples such as the subject of Figure 8, in which the image quality is so degraded that a consistent layer of ink is never achieved. It is, however, useful as a tool to determine an estimate of the point at which it is most critical to quantify the granularity of printing systems such as those studied herein.

Summary and Conclusions

Given the current state-of-the-art, the halftoned image view quality of solid ink prints is influenced by a different set of

parameters than the view quality of xerographic prints. Ignoring mechanical anomalies such as banding and concentrating on technology issues, in the case of solid ink, the maximum granularity is governed primarily by the size and contrast of the minimum mark. While it is possible enhance image quality through the use of some highly uniform specialty medias, it is rare that receiver media choice causes customer rejection on the basis of poor image view quality. In xerography, more often the opposite is true. The minimum mark size is rarely the limiting factor in image quality. Usually, in cases of questionable print quality on non-coated papers, artifacts result from poor formation and/or high surface roughness of the paper.

An analysis of granularity and optical density revealed that maximum granularity of a binary halftoned print occurs at the point in which half the pattern area is covered with ink. Although this fact was determined empirically, it is supported by the statistics of binomial distributions. Dot gain effects cause this point to occur well below 50% digital coverage in both solid ink and xerographic systems. Further effects of dot gain result in complete area coverage of the paper well before maximum optical density is achieved. This is especially true of solid ink systems in which hemispherical dots are physically smashed into platelets via the image transfer/fixing process. This is an important point, as once this complete layer of ink has been deposited, the contrast is greatly reduced and the noise contribution of the dithering process is attenuated with a corresponding decrease in granularity.

Acknowledgments

References

1. Shaw, R., Image Quality Considerations for Printing Digital Photographs, Proceedings of IS&T's NIP 13, (1997).
2. McGuire M., Shaw, R., Autocovariance Techniques for the Practical Evaluation of Digital Image Noise, Proceedings of IS&T's NIP 13, (1997).
3. Sakatani, K., Hirota, S., and Itoh, T., Graininess Metric for Digital Halftone Images, Proceedings of IS&T's NIP 12, (1996).
4. Snyder, T., Korol, S., Modeling the Offset Solid Ink Printing Process, Proceedings of IS&T's NIP 13, (1997).
5. Ulichney, R. Digital Halftoning. MIT Press, Cambridge, Massachusetts, (1987).
6. Schaffert, R.M., Electrophotography, Second Edition. Focal Press Limited, London, England, (1975).
7. Schein, L.B., Electrophotography and Development Physics. Springer-Verlag, Heidelberg, Germany, (1988).
8. Burns, P.D. Measurement of Random and Periodic Image Noise in Raster-Written Images, Proceedings of the SPSE Advances in Non-Impact Printing Technologies, (1984).
9. Dainty, J.C., Shaw, R., Image Science, Academic Press, San Diego, California, (1974).
10. Gonzalez, R.C., Woods, R.E., Digital Image Processing, Addison-Wesley, Reading, Massachusetts, (1992).
11. Yule, J.A., Nielsen, W.J., TAGA, p. 65, (1951).